

Electrically tunable wettability of liquid crystal/polymer composite films

Yi-Hsin Lin¹, Hongwen Ren², Yung-Hsun Wu², Shin-Tson Wu²,
Yue Zhao³, Jiyu Fang³, and Hung-Chun Lin¹

¹Department of Photonics and Institute of Electro-Optical Engineering, National Chiao Tung University,
1001 Ta Hsueh Rd., Hsinchu 30050, Taiwan

²College of Optics and Photonics, University of Central Florida, Orlando, Florida 32816, USA

³Advanced Materials Processing and Analysis Center and Department of Mechanical, Materials and Aerospace
Engineering, University of Central Florida, Orlando, Florida 32816, USA

yilin@mail.nctu.edu.tw

<http://www.cc.nctu.edu.tw/~yilin>

Abstract: An electrically tunable wettability in a liquid crystal/ polymer composite film is demonstrated, in which liquid crystal molecules are anchored among polymer grains. The tunable wettability of the composite films originates from the reorientation of the anchored liquid-crystal molecules, which is switched by an in-plane electric field with squared pulses of voltages. These liquid crystal/polymer composite films with electrically tunable wettability have potential applications in polarizer-free displays, ink-jet printing, microfluidic devices, and lab-on-a-chip.

©2008 Optical Society of America

OCIS codes: (230.3720) Liquid-crystal devices; (160.5470) Polymers.

References and links

1. T. P. Russel, "Surface-responsive materials," *Science* **297**, 964-967 (2002).
2. Y. Liu, L. Mu, B. Liu, and J. Kong, "Controlled switchable surface," *Chem. Euro. J.* **11**, 2622-2631 (2005).
3. S. L. Gras, T. Mahmud, G. Rosengarten, A. Mitchell, and K. Kalantar-zadeh, "Intelligent control of surface hydrophobicity," *Chemphyschem.* **8**, 2036-2050 (2007).
4. X. Feng and L. Jiang, "Design and creation of superwetting/antiwetting surfaces," *Adv. Mater.* **18**, 3063-3078 (2006).
5. M. Motornov, R. Sheparovych, R. Lupitskyy, E. MacWilliams, and S. Minko, "Responsive colloidal systems: Reversible aggregation and fabrication of superhydrophobic surfaces," *J. Colloid Interface Sci.* **310**, 481-488 (2007).
6. A. Sidorenko, T. Krupenkin, A. Taylor, P. Fratzl, and J. Aizenberg, "Reversible switching of hydrogel-actuated nanostructures into complex micropatterns," *Science* **315**, 487-490 (2007).
7. R. Rosario, D. Gust, A. A. Garcia, M. Hayes, J. L. Taraci, T. Clement, J. W. Dailey, and S. T. Picraux, "Lotus effect amplifies light-induced contact angle switching," *J. Phys. Chem. B* **108**, 12640-12642 (2004).
8. M. Riskin, E. Katz, V. Gutkin, and I. Willner, "Photochemically controlled electrochemical deposition and dissolution of Ag nanoclusters on Au electrode surfaces," *Langmuir* **22**, 10483-10489 (2006).
9. Y. Jiang, P. Wan, M. Smet, Z. Wang, and X. Zhang, "Self-assembled monolayers of a malachite green derivative: surfaces with pH- and UV-responsive wetting properties," *Adv. Mater.* **20**, 1972-1977 (2008).
10. E. Bormashenko, R. Pogreb, G. Whyman, Y. Bormashenko, R. Jager, T. Stein, A. Schechter, and D. Aurbach, "The reversible giant change in the contact angle on the polysulfone and polyethersulfone films exposed to UV irradiation," *Langmuir* **24**, 5977-5980 (2008).
11. G. de Crevoisier, P. Fabre, J. Corpart, and L. Leibler, "Switchable tackiness and wettability of a liquid crystalline polymer," *Science* **285**, 1246-1249 (1999).
12. J. Lahann, S. Mitragotri, T. Tran, H. Kaido, J. Sundaram, I. S. Choi, S. Hoffer, G. A. Somorjai, and R. Langer, "A reversibly switching surface," *Science* **299**, 371-374 (2003).
13. D. Kaneko, K. Shibata, T. Kaneko, and Y. Kawakami, "Transportation of a microdroplet on an oriented liquid crystal surface," *Liq. Cryst.* **35**, 661-664 (2008).
14. Y. H. Lin, H. Ren, Y. H. Wu, Y. Zhao, J. Fang, Z. Ge, and S. T. Wu, "Polarization-independent phase modulator using a thin polymer-separated double-layered structure," *Opt. Express* **13**, 8746-8752 (2005).
15. Y. H. Lin, H. Ren, S. Gauza, Y. H. Wu, and S. T. Wu, "Single-substrate IPS-LCD using an anisotropic polymer film," *Proc. SPIE* **5936**, 59360O (2005).
16. Y. H. Lin, H. Ren, S. Gauza, Y. H. Wu, Y. Zhao, J. Fang, and S. T. Wu, "IPS-LCD using a glass substrate and an anisotropic polymer film," *J. Disp. Technol.* **2**, 21-25 (2006).

17. M. Ibn-Elhaj and M. Schadt, "Optical polymer thin films with isotropic and anisotropic nano-corrugated surface topologies" *Nature* **410**, 796-799 (2001).
18. T. B. Jones, J. D. Fowler, Y. S. Chang, and C. J. Kim, "Frequency-based relationship of electrowetting and dielectrophoretic liquid microactuation," *Langmuir* **19**, 7646-7651 (2003).
19. P. G. de Gennes, "Wetting: statics and dynamics," *Rev. Mod. Phys.* **57**, 827-863 (1985).
20. J. Bico, C. Tordeux, and D. Quere, "Rough wetting," *Europhys. Lett.* **55**, 214-220 (2001).
21. D. Quere, "Rough ideas on wetting," *Physica A*, **313**, 32-46 (2002).
22. R. N. Wenzel, "Resistance of solid surfaces to wetting by water," *Ind. Eng. Chem.* **28**, 988-994 (1936).
23. T. Young, "An essay on the cohesion of fluids," *Phil. Trans. R. Soc. Lond.* **95**, 65-87 (1805).
24. A. B. D. Cassie and S. Baxter, "Wettability of porous surface," *Trans. Faraday Soc.* **40**, 546-551 (1944).

1. Introduction

Tunable wettability of designed surfaces has many applications, such as automobile windshield, polarizer-free display, ink-jet printing, microfluidic device, and lab-on-a-chip. Many switchable surfaces based on polymers have been demonstrated [1-4], including surface modification by surrounding media [2-6], photon-induced surface modification [1-3, 7-10], electrochemical surface modification [1-3], and thermo-switchable surface [2, 3, 4 11]. In addition, switchable surfaces based on self-assembled monolayers (SAMs) also attract many attentions [2, 3, 12]. A microdroplet transportation on an inhomogeneous liquid crystal (LC) fluid has been demonstrated [13]; however, the fluid nature of LC limits the applications. Recently, we have developed an LC/polymer composite film using a phase separation process to make a double-layered LC phase modulator [14] and a single-substrate in-plane switching (IPS) liquid crystal display [15, 16]. The LC/polymer composite film can also be used as an alternative substrate as well as an alignment layer [14-16].

In this paper, we demonstrate an electrically tunable wettability in the LC/polymer composite film by controlling the orientation of LC molecules anchored among the polymer grains. The contact angle of a water droplet on the LC/polymer composite films at room temperature can be switched in the range between 65° and 80° by an in-plane electric field. To prove concept, an adaptive-focus liquid lens using this electrically tunable wettability is demonstrated.

2. Sample preparation and operating principle

Figures 1(a) and 1(b) depict the device structure and operating principles of the electrically tunable wettability system. The device consists of an LC/polymer composite film on an IPS glass substrate overcoated with a patterned ITO (indium tin oxide) electrode. The ITO electrode on the glass substrate was etched with interdigitated chevron patterns. The angle of the zigzag ITO stripes is 160°. The width and gap of the electrode stripes are 4 μm and 10 μm, respectively. The zigzag ITO electrode stripes generate in-plane electric fields.

To fabricate the LC/polymer composite film [14-16], we mixed a nematic LC mixture E7 (Merck) and a liquid crystalline monomer (4-(3-Acryloyloxypropyloxy)-benzoic acid 2-methyl-1, 4-phenylene ester) at 60:40 wt % ratios. The LC/monomer mixture shows a nematic phase between -20 °C and 80 °C. We prepared an empty cell with a gap of 12 μm which consists of a top glass substrate (without ITO) and a bottom substrate with IPS electrodes. The top substrate was overcoated with a thin polyimide layer and then mechanically buffed at +10° with respect to the y-axis. As shown in Fig. 1(b), the bottom electrode stripes are along the y-axis. The cell filled with the LC/monomer mixture was exposed to a unpolarized UV light with a homogeneous intensity $I = 10 \text{ mW/cm}^2$ for ~30 min at 70 °C. The UV incidence was on the side of the top substrate. As a result, the patterned electrodes on the bottom substrate did not affect the phase separation process. After phase separation and photo-polymerization, the top glass substrate was peeled off by a thermal release process, leading to the formation of a solidified and uniaxial LC/polymer composite film of 12-μm thickness, as depicted in Fig. 1(a). The uniaxial polymer topologies induced by the uniaxial phase separation are because the LC molecules and LC monomers are aligned by the rubbed PI layers before photo-polymerization and the polymer grains of the LC/polymer composite film aggregates and elongates along the rubbing direction after phase separation. The mechanism is analogous to

the nano-corrugated surface topologies published by Ibn-Ehlhaj et. al [17]. When we peel off the top glass substrate and leave the LC/polymer composite film on the other substrate during fabrication process, the LC molecules stay on the both surfaces, the surface on the top substrate and the surface on the LC/polymer composite film, and then leave the anisotropic topologies with valleys and polymer network structures. To see the LC/polymer composite film surface more clearly, we magnify a portion of Fig. 1(a) as shown in Fig. 1(b). At $V=0$, the LC directors are aligned almost along y-direction, parallel to the rubbing direction. Under applied a.c. voltage ($f = 1$ kHz), the LC directors are reoriented by the electric fields.

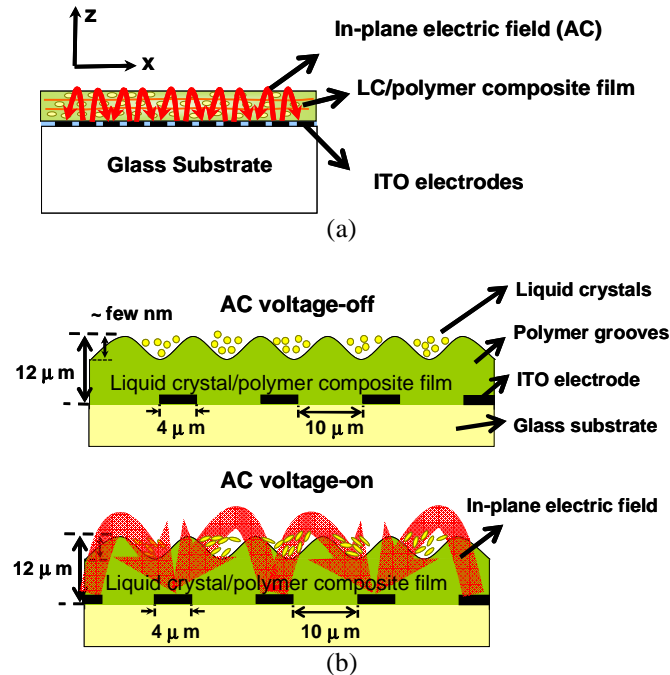


Fig. 1. (a) Schematic of the device structure of the LC/polymer composite film and (b) the magnified surface of the LC/polymer composite film at voltage-off and voltage-on states.

3. Experiment and results

The LC/polymer films were imaged with an atomic force microscope (AFM) (Dimension 3100, Digital Instruments) at tapping mode at room temperature in air. Silicon nitride cantilevers (Nanosensors) with a resonant frequency of 260 kHz were used. The cantilevers were excited just below its resonant frequency. The apical radius of the cantilevers is about 15 nm. The AFM images of liquid crystal/polymer films with different LC concentrations are shown in Figs. 2(a)-2(d). As can be seen, the surface of the LC/polymer films shows elongated aggregation of polymer grains along the rubbing direction (indicated by arrows). The root-mean-square (RMS) roughness of the films surfaces is 1.5 nm at 10 wt% LC, 1.0 nm at 20 wt% LC, 1.5 nm at 30 wt% LC, and 5.0 nm at 40 wt% LC, respectively.

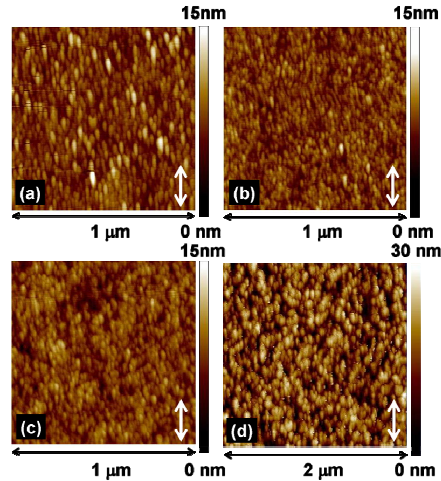


Fig. 2. AFM images of the LC/polymer composite film at (a) 10 wt% LC, (b) 20 wt% LC, (c) 30 wt% LC, and (d) 40 wt% LC.

To verify the LC directors anchored between polymer grains can be switched by the in-plane electric fields, we observed the LC/polymer films on the top of an IPS glass substrate (Fig. 1(a)) by using a polarizing optical microscope. The polarizer (P) and analyzer (A) are orthogonal to each other and the rubbing direction of the bottom IPS substrate is parallel to the transmission axis of the polarizer. As shown in Fig. 3, at $V=0$ V_{rms} the LC directors and polymer grains tend to align along the direction of the transmission axis of the polarizer. However, the LC/polymer film still has a small light leakage because the LC directors and polymer grains are not perfectly aligned along the same direction. At 200 V_{rms} at $f = 1$ kHz, the transmission of the LC/polymer film increases because of the birefringence effect induced by the LC reorientation.

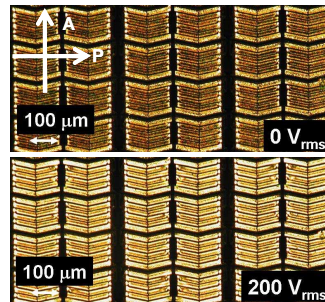


Fig. 3. Microscopic photos taken from a polarizing microscope with crossed polarizers at 0 V_{rms} and 200 V_{rms} . “P” indicates the transmission axis of the polarizer and “A” indicates the transmission axis of the analyzer.

To observe the dynamic wettability of the LC/polymer films under in-plane electric fields, we carried out contact angle measurements using a CCD camera, as shown in Figs. 4(a) and 4(b). The CCD camera was looking at the water contact angle along the y-axis as Fig. 1 shows (or P-direction in Fig. 3). A 3 μl drop of de-ionized water was deposited on the LC/polymer films. The droplet covers over 500 electrode stripes. We applied 200 V_{rms} squared pulses ($f = 1$ kHz) to the LC/polymer film (with 60 wt% LC) for 600 ms.

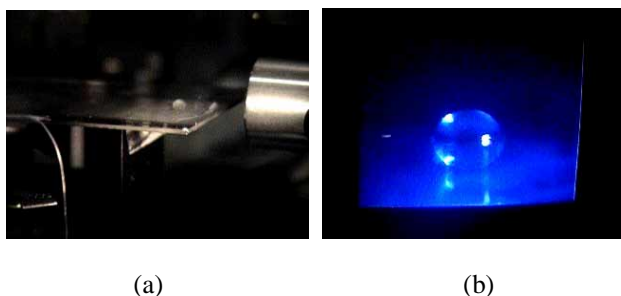


Fig. 4. (a) Contact angle measurement (Media 1), and (b) the image observing by CCD: the side view of water droplet on the top of LC/polymer film under 200 V_{rms} squared pulses ($f = 1$ kHz) observed through a CCD camera (Media 2).

Figure 5 shows the measured results. We did measurements 6 times at different locations of each film and the averaged water contact angle changes periodically between 80.65° and 64.10° with periodically applied electric fields. The experimental error is ± 2.5 degree. The contact angle fluctuation at the period of 0 V_{rms} and of 200 V_{rms} is a result of the elastic bounce of the water droplet under voltage-on and voltage-off. The response time was defined as the total time duration of contact angle transition from the high degree to the low degree and then from the low degree to the high degree. It was found to be around 400 ms.

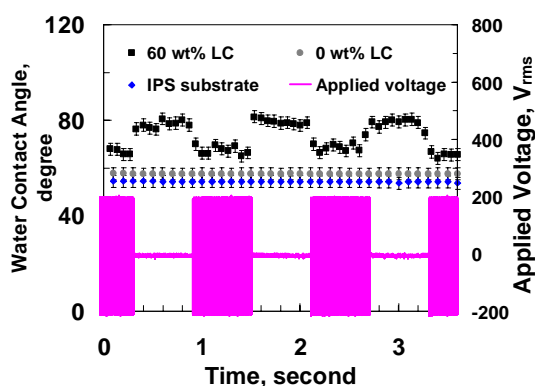


Fig. 5. Water contact angle as a function of time under a squared pulsed voltage (200 V_{rms}) with 600 ms time duration for the LC/polymer composite films with 60 wt% LC and 0 wt% LC, and the IPS glass substrate.

In addition, the water contact angle on the LC/polymer film is electrically tunable. In Fig. 6, the difference between the maximal and minimal contact angles increases when we increase the amplitude of squared pulses of an in-plane electrical field with a fixed time duration at $f = 1$ kHz from 100 V_{rms} to 200 V_{rms} at 60 wt% LC. The threshold voltage is around 100 V_{rms}. The total angle change is 2° at 100 V_{rms} (between 79° and 81°), 5° at 140 V_{rms} (between 75° and 80°), and 15° at 200 V_{rms} (between 65° and 80°).

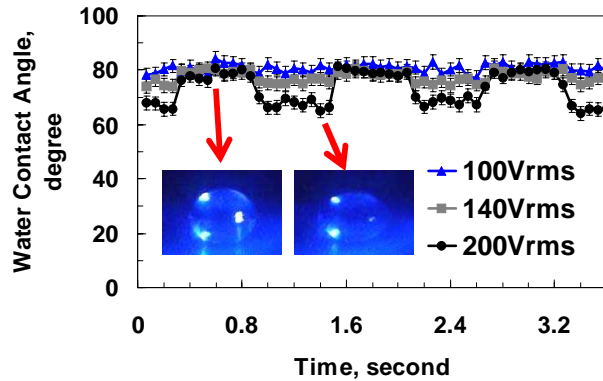


Fig. 6. Water contact angle of the LC/polymer composite film with 60 wt% LC as a function of time under different squared pulsed voltage with 600 ms time duration. ($f = 1$ kHz)

To prove that the contact angle change results from the reorientation of the LC directors anchored among the polymer grains, we carried out the water contact experiments on pure polymer films without LC molecules. The water contact angle was found to be 57.63° . We also measured the water contact angle on the top of IPS glass substrate without LC/polymer film and it was found to be 54.45° . The measured water contact angle on the pure polymer film without LC molecules does not change with squared pulses of an in-plane electric field with a fixed time duration at $f = 1$ kHz, as shown in Fig. 5. Without LC, the surfaces, pure polymer film and IPS glass substrate, are more hydrophilic. Such surfaces are not suitable for electrostatic actuation. However, the water contact angle on the LC/polymer film with 60 wt% LC changes periodically with a periodically applied voltage even though the macroscopic surface is more hydrophilic. So we conclude that the orientation change of the LCs anchored between polymer grains in responding to the electric fields leads to the observed dynamic change of surface wettability. The electrostatic force can be neglected for two reasons: 1) the LC/polymer film is not operated in high-frequency-limit region (>10 kHz) in which dielectrophoretic (DEP) effect has influence on water droplet [18], and 2) the LC/polymer film is thick (about $12 \mu\text{m}$), therefore, the electric field near the water-film surface is relatively weak to stretch the droplet using DEP, but it is strong enough to change LC orientations.

One application of LC/polymer film is the dynamic liquid lens, as Fig. 7 shows. A water droplet of $\sim 6 \mu\text{l}$ was put on the top of the clear LC/polymer film and electrodes. The distance between the image and the substrate is 2 mm. The focal length changes periodically with the applied pulsed voltages. The measured focal length of the liquid lens is 4.2 mm at $0 V_{\text{rms}}$ and 5.3 mm at $200 V_{\text{rms}}$. In Fig. 7, the contact angle change is along the direction of the in-plane electric fields. In addition, the images inside the water droplet area have different magnification with applied electric field. This is because the contact angle change results in a change on the water droplet curvature which, in turn, leads to a focal length change.

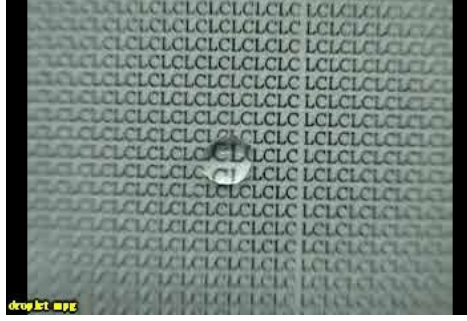


Fig. 7. The top view of water droplet on a LC/polymer composite film under squared pulsed voltage ($200 V_{rms}$) with 600 ms time duration. ($f = 1$ kHz) A paper with printed images was put right behind the glass substrate ([Media 3](#)).

5. Discussion

It is known that several factors can affect surface wettability, such as chemical properties of the materials, roughness, and chemical heterogeneity [19-21]. The effect of the roughness can be described by the Wenzel's relationship [22]:

$$\cos(\theta_1) = R_w \cdot \cos(\theta_2), \quad (1)$$

where R_w is the surface roughness factor, θ_2 is the contact angle in the smooth surface and θ_1 is the contact angle in a rough surface. Equation (1) describes the amplification of surface properties due to the surface roughness. The contact angle θ_2 satisfies Young's equation [23]:

$$\cos(\theta_2) = \frac{\gamma_{SV} - \gamma_{SL}}{\gamma_{LV}}, \quad (2)$$

where γ represents the surface tension (i.e., energy per unit surface) of the interface, and S, L, and V indicate the phases of the solid, liquid and vapor. When a surface has the chemical heterogeneity and surface porosity, the contact angle (θ) of modified Cassie's equation can be expressed as [24]:

$$\cos(\theta) = f_3 \cdot \cos(\theta_3) + f_4 \cdot \cos(\theta_4), \quad (3)$$

where f_3 and f_4 are the fractions of the surface having inherent contact angles θ_3 and θ_4 . Here, f_3 and f_4 should satisfy: $f_3 + f_4 = 1$. However, the water contact angle on the LC/polymer composite film depends not only on the morphologies (both polymers and liquid crystals) but also on the orientation of LC directors which can be controlled by the applied electric fields. Thus, the contact angle (θ') as a function of applied voltage (V_{rms}) in the LC/polymer composite film should be:

$$\cos[\theta'(V_{rms})] = f_{lc} \cdot \cos(\theta_{lc}(V_{rms})) + f_p \cdot \cos(\theta_p), \quad (4)$$

$$\cos(\theta_{lc}(V_{rms})) = \frac{\gamma_{lc,V}(V_{rms}) - \gamma_{lc,L}(V_{rms})}{\gamma_{LV}}, \quad (5)$$

where f_{lc} and f_p are the fractions of LC and polymer grains for the inherent contact angles θ_{lc} and θ_p , respectively. From Eq. (5), when the voltage is higher than the threshold voltage, $\gamma_{lc,L}(V_{rms})$ is smaller than $\gamma_{lc,L}(0)$, because the tilts of the terminal groups of LC directors near the edge of the electrodes have a lower surface tension. By assuming $\gamma_{lc,V}(V_{rms}) \approx \gamma_{lc,V}(0)$, we

can infer that $\theta_{lc}(V_{rms})$ is smaller than $\theta_{lc}(0)$ because $\cos(\theta_{lc}(V_{rms})) > \cos(\theta_{lc}(0))$. Therefore, the surface wettability of the LC/polymer composite film is electrically switchable.

6. Conclusion

We have demonstrated electrically tunable wettability of an LC/polymer composite film, in which LC molecules are anchored among polymer grains. The LC reorientation among polymer grains at the LC/polymer composite film surfaces, which are switched by the electric field, is responsible for the observed tunable wettability of the LC/polymer composite film. The major advantages of LC/polymer composite film are threefold: 1) small Joule's heating which is a common issue for DEP or electrowetting in water-based devices, 2) small hysteresis, and 3) low power consumption. The mechanism of DEP is to apply an inhomogeneous electric field to a dielectric liquid to generate a pulling force which changes the contact angle of the droplet. On the contrary, the wettability change of a LC/polymer composite film is because the molecular orientation anchored the polymer grains of the surface. The electrically switchable wettability of LC/polymer composite films has potential applications in liquid lens, windshield, polarizer-free displays, ink-jet printing, microfluidic devices, and lab-on-a-chip.

Acknowledgments

The authors are indebted to Prof. Shu-Hsia Chen of National Chiao Tung University (Taiwan) and Dr. Chih-Chung Cheng in ITRI (Taiwan) for discussions, Chi Mei Optoelectronics (Taiwan) for providing glass substrates, and Jiong-Kuan Li, Ting-Yu Chu and Chih-Ming Yang for technical assistance. This research was supported by the National Science Council (NSC) in Taiwan under the contract no. 96-2112-M-009-019-MY2.